
**SYNTHESIS AND PROPERTIES
OF INORGANIC COMPOUNDS**

Effects of Amino Acids on the Composition and Particle Size of Calcium Carbonate Precipitated in Bile

S. S. Leonchuk^{a,*} and O. A. Golovanova^a

^a Omsk State University, Omsk, 644050 Russia

*e-mail: ssleonchuk@yandex.ru

Received August 9, 2021; revised October 11, 2021; accepted October 13, 2021

Abstract—Calcium carbonate crystallization was experimentally modeled in a model human bile solution. CaCO₃ samples were prepared in the presence of variable concentrations of histidine (His), arginine (Arg), methionine (Met), or tryptophan (Trp). The phase and structure-group compositions of the prepared samples were determined by X-ray powder diffraction and FT-IR spectroscopy. CaCO₃ percentages, particle sizes, and volume proportions of various size fractions in the prepared powders were determined. The samples prepared in the presence of Arg have the highest yield as impurity-free CaCO₃; those prepared in the presence of Met have the lowest yield. The increasing amino acid (AA) concentration gives rise to an increase in the calcium carbonate weight fraction in the syntheses with His or Arg and to a decrease in the syntheses with Met or Trp. The major component of the phase composition in all of the prepared powders is represented by vaterite, a metastable CaCO₃ polymorph. The proportion of the aragonite fraction in the solid increases as the Arg or Met concentration in bile increases. Calcium carbonate microparticles with radii less than 10 μm are represented by three fractions. As the His or Trp concentration in the model bile solution increases, the proportion of the small-size fraction increases while the proportion of the coarse-size fraction decreases, with the particle radii increasing in all fractions.

Keywords: vaterite, aragonite, calcite, synthesis, phase composition, particle size, crystallization, gallstones

DOI: 10.1134/S0036023622040118

INTRODUCTION

Calcium ions play an important role in many biochemical and bioinorganic processes in the human body; they occupy a special place in the mineralization of bone and dental tissues, as well as in pathogenic mineralization processes [1–3]. The relevance of studying these processes can hardly be overvalued, for a whole line of research that concerns pathological crystals has been formed in modern materials science over the past few decades [4].

Such the crystals include gallstones (choleliths), whose formation in the human body leads to gallstone disease (cholelithiasis). The bile composition and concentrations of bile components play important roles in these processes [2, 5, 6]. Of particular importance in gallstone formation is the formation of calcium carbonate microcrystals, whose properties (phase composition, morphology, and particle size) are closely related to the crystallization of cholesterol from bile and, as a result, to the growth of choleliths, which is the key factor in gallstone formation [1, 2, 6]. This fact is also verified by recent studies of calcium carbonate crystallization, according to which spontaneous cholesterol nucleation is impossible in the absence of inorganic calcium salts, for it requires

~300% solution supersaturation. Such a cholesterol concentration in human bile is physiologically impossible; therefore, cholesterol nucleation is a result of heterogeneous crystallization with the participation of calcium carbonate and calcium bilirubinate [1, 7, 8].

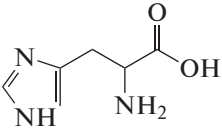
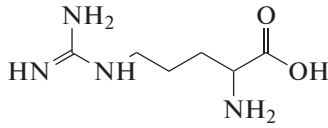
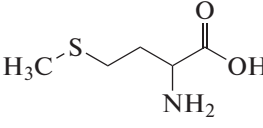
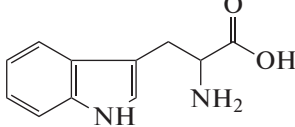
Normally, the human bile contains both inorganic components (ions) and organic components (bile acids, lecithin, cholesterol, bilirubin, etc.), which constitute the basis of the dry residue [3, 9, 10].

Calcium carbonate, which is naturally polymorphic, can exist in three crystal polymorphs: calcite (stable), aragonite, and vaterite (the last two are metastable) [11].

Importantly, the major phase in the inorganic component of gallstones is precisely a metastable calcium carbonate polymorph, namely, vaterite, while aragonite and calcite are contained in choleliths in trace amounts, directly due to the conditions of CaCO₃ crystallization [4–7, 12, 13].

Mathematical modeling shows that the amino acids histidine (His), arginine (Arg), methionine (Met), and tryptophan (Trp) in the peptide have strong interfacial Ca–O bonds and O··H hydrogen bonds with the (001) aragonite surface [14]; that is,

Table 1. Amino acids studied [19, 21]

Name, abbreviation	Structural formula	FW, g/mol	C_{avg} , $\mu\text{mol/L}$	C_{mod} , mmol/L
Histidine, His (H)		155.16	123	1.23
Arginine, Arg (R)		174.20	132	1.32
Methionine, Met (M)		149.21	27	0.27
Tryptophan, Trp (W)		204.23	60	0.60

theoretically, they can stabilize this polymorph upon CaCO_3 precipitation from solution.

However, theoretical calculations require experimental confirmation. Of interest is the effect of these amino acids on calcium carbonate precipitated from bile, because, as mentioned above, it is vaterite that usually forms under these conditions. The transfer of CaCO_3 to another phase upon in vivo crystallization in the human body can reduce the stability of the newly formed microparticles, can lead to inhibition of cholesterol crystallization. It is also known that various biliary pathologies (including cholelithiasis) involve a change in the bile and blood levels of amino acids [15].

A detailed study of the mechanism of and conditions for in-vivo CaCO_3 crystallization in the human body can be via experimental modeling, namely, the synthesis and analysis of the prepared samples [2, 16–20]. Some methods for the synthesis of inorganic calcium compounds are also used in nanomaterials design [21–24].

The goal of this work was an experimental study of the effects of variable concentrations of the amino acids histidine (His), arginine (Arg), methionine (Met), and tryptophan (Trp) on the composition and properties of calcium carbonate precipitated from bile.

EXPERIMENTAL

Selection of Model Concentrations

Model concentrations. The concentration of free amino acids (AAs) in human bile depends on their concentration in blood plasma and, as a rule, has close

values [25]. Hood et al. [26], in their studies of the stabilizing activity of amino acids with respect to vaterite formation from aqueous solutions, used those AAs in concentrations of 10–50 mmol/L, i.e., one to two orders of magnitude higher than the plasma level of AAs.

To improve the accuracy and reproducibility of the results of experimental modeling in the synthesis of CaCO_3 , we used model concentrations of Ca^{2+} , HCO_3^- , and amino acids 10 times as high as the respective average concentrations in the human bile. This proportionate increase maintains the concentration ratios between the compounds studied, while not exceeding the total ionic strength of the bile solution, which normally contains other ions too, and allows one to carry out the synthesis of CaCO_3 in small volumes.

As mentioned above, our study will consider only the four amino acids that are of interest in terms of their effect on CaCO_3 crystallization and phase formation. For convenience, Table 1 compiles selected information on these AAs.

The reagents used for the synthesis of calcium carbonate were sodium bicarbonate and calcium chloride dihydrate, as the most suitable in terms of the chemical composition of the human bile. Their concentrations referred to the model conditions appear in Table 2.

Calcium Carbonate Synthesis

Experiment plan. The study of the effects of amino acids on CaCO_3 crystallization involved variations of model AA concentrations while constant Ca^{2+} and

Table 2. Characteristics of reagents

Reagent (formula)	Ion added	FW, g/mol	C_{avg} (ion), mmol/L	C_{mod} (ion), mol/L
NaHCO ₃	HCO ₃ ⁻	84.01	10	0.10
CaCl ₂ ·2H ₂ O	Ca ²⁺	147.01	12	0.12

Table 3. Codes of CaCO₃ samples with AAs

No.	1	2	3	4	5
$C(\text{AA})$	$0.5C_{\text{mod}}$	$1C_{\text{mod}}$		$2C_{\text{mod}}$	$10C_{\text{mod}}$
$V(\text{synthesis}), \text{mL}$	200	200	100	200	200
Amino acid	Name of the CaCO ₃ sample				
His (H)	H1	H2	H3	H4	H5
Arg (R)	R1	R2	R3	R4	R5
Met (M)	M1	M2	M3	M4	M5
Trp (W)	W1	W2	W3	W4	W5

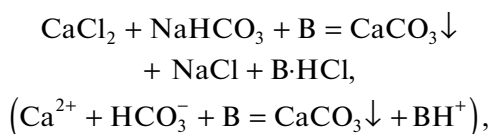
C_{mod} is the model amino acid concentration.

HCO₃⁻ model concentrations and constant pH were maintained in the reaction mixture. Variation of AA concentration involved a manifold change in the model concentration by 0.5, 2, and 10 times (Table 3). Syntheses 2 and 3 differed from each other only by volumes, the other conditions being equal; this was necessary for verifying the reproducibility of results of experimental modeling. Thus, five CaCO₃ samples were prepared to study the effect of every amino acid. Two CaCO₃ samples were prepared in the absence of amino acids, with the other conditions being equal.

Since the experiment involved the preparation of a large number of samples of the same type, we encoded their names. To each synthesis (sample), there were assigned a specific serial number (in the increasing order of concentrations) and a letter (one-letter designation of the amino acid used in the synthesis); see Table 3.

General synthetic scheme. Before the synthesis, a model solution of bile was prepared: dry bile for biochemistry (bovine bile dry, purified, TU 10.02.01.112-89, Omskreaktiv) was dissolved in distilled water to provide a concentration of 105 g/L.

The CaCO₃ synthesis followed the equation



where B stands for the organic base in the bile.

The major synthetic stages were as follows:

(1) Preparation of the model bile solution (200 or 100 mL).

(2) Division of the model bile solution into two equal parts (solutions 1 and 2).

(3) Addition of the required amount of NaHCO₃ to solution 1 and CaCl₂·2H₂O and an amino acid to solution 2.

(4) Addition of solution 1 from burette to solution 2 on a magnetic stirrer, stirring for 10 min, and adjusting pH to 7.0 (with 2 M NaOH or HCl 1 : 1).

(5) Addition of formalin to provide 1% formaldehyde concentration in the resulting solution (for the preservation of bile).

(6) Exposure of the thus-prepared solution in a BIOTRON-4 drying cabinet for 7 days at 310 ± 1 K.

(7) Vacuum filtration; the precipitate on the filter was washed twice with distilled water, 50 ml each time.

(8) Drying of the precipitate for 24 h in a Biotron-4 drying cabinet at 310 ± 1 K, then for 24 h in a desiccator at room temperature to constant weight (to remove all chemically unbound water).

(9) Weighing of the dehydrated dry powder to determine the yield, followed by its characterization by physicochemical methods.

X-ray powder diffraction (XRD) experiments were carried out on a DRON-3M diffractometer using CuK_α radiation in the 2θ angle range from 10° to 60° with 0.2° steps. The qualitative and quantitative analyses of the phase composition of a sample were in the Match! 3 (Crystal Impact) software based on the COD (2020) crystallographic database. The MS Excel 2019 and OriginPro 2021 programs were used for the graphic representation of the X-ray diffraction patterns.

FT-IR spectra of the prepared powders were recorded as KBr disks on an FSM-2202 (Infraspek) spectrophotometer using the FSpec software. The resolution was 4 cm^{-1} ; the scan range was from 400 to 4000 cm^{-1} . The IR spectra were processed in MS Excel 2019 and OriginPro 2021 programs using the SDBS (Aist) and ICSD (Nist) spectral databases and documented IR spectra of inorganic compounds [9, 28–31].

Optical microscopy of the prepared samples was fulfilled using an XSZ-107 (Armed) microscope equipped with a TouPCam (TouPTek) camera with 3.1 MP, and TouView software.

Hydrodynamic particle radii in the prepared samples were determined by photon correlation spectroscopy (PCS) on a Photocor Compact (Photocor) particle size analyzer using the program package comprised of Photocor-FC to manage measurements and DynaLS for subsequent processing of correlation functions (GOST (State Standard) R 8.774-2011). The liquid used to prepare suspensions of the test powders was distilled water purified by a Chromafil Xtra PET (Macherey-Nagel) syringe filter with 200-nm pores. The concentration of the analyzed suspensions was 0.1 mg/mL . The powders were dispersed in an Ultrasonic Cleaner JP-010S (Skymen) ultrasonic bath at a frequency of 40 kHz for 10 min.

Ca^{2+} concentration in the solid was determined as CaCO_3 by complexometric titration of prepared powders after the samples were solubilized by the procedure based on GOST (State Standard) 21138.5-78 and GOST (State Standard) 23268.5-78 and adapted to the subject matter. The MS Excel 2019 and OriginPro 2021 programs were used for data processing.

RESULTS AND DISCUSSION

The calcium percentage as impurity-free stoichiometric CaCO_3 in the prepared samples was determined by complexometric titration. The data were statistically processed; they are presented in Table 4 as confidence intervals. For each series of syntheses, the results were verified by one-way analysis of variance, which reliably established correlation relations.

The calcium carbonate percentage is variable. In the syntheses with His or Arg, the CaCO_3 percentage in the solid increases as the amino acid concentration in bile increases. This trend can be due to the basicity of these amino acids. Met and Trp have no common features in their structures or acid–base properties, but they exhibit a similar effect toward calcium carbonate: the calcium carbonate percentage in samples decreases in response to increasing concentration of either of these amino acids; that is, they inhibit CaCO_3 crystallization.

For the syntheses with Met and Arg, $\omega(\text{CaCO}_3)$ is an exponential function of AA concentration in bile;

this can be seen from the correlation coefficients when such a dependence is superimposed on the datapoints (Fig. 1).

Qualitative XRD showed vaterite as the major phase in all samples; the peaks at $2\theta = 24.9^\circ$, 27.0° , 32.7° , 44.5° , and 50.0° are the strongest and visually distinguishable. Aragonite ($2\theta = 26.3^\circ$, 27.3° , 38.5° , 33.2° , 36.2° , 43.0° , 46.0° , etc.) and calcite ($2\theta = 29.4^\circ$, 39.5° , 43.1° , 48.5° , etc.) were also found in all powders, but in far lower amounts. The X-ray diffraction patterns of all synthesized CaCO_3 samples are almost identical, differing from one another only by a small set of peaks and their relative intensities. Figure 2 shows X-ray diffraction patterns for powders prepared in the presence of arginine. One can notice the shifts of characteristic reflection angles toward the smaller 2θ angles (the greatest shift is $\sim 1.5^\circ$) for all synthetic lines, with the general diffraction pattern remaining unchanged as the amino acid concentration in bile rises; this trend signifies an increase in interplanar spacings in the crystal structure of nascent CaCO_3 phase. This can be due to the incorporation of bulky anions of amino acid residues into the calcium carbonate crystal structure.

The more detailed quantitative XRD determined the vaterite, aragonite, and calcite percentages in the crystalline phase. In Table 5, one can see the trend of the aragonite percentage in the powders.

Of interest is a correlation (reliably established drift) between the aragonite percentage in the solid phase and the amino acid concentration in bile for the syntheses with Met or Arg: the amount of the aragonite phase increases as the concentration of either of these amino acids rises. For CaCO_3 samples with His, an opposite trend is observed. The synthesis with Trp in bile do not feature such a correlation.

The FT-IR results correlate with previous analyzes. The IR spectra of the prepared samples feature all characteristic vibrations of the CO_3^{2-} : triangular ion: the non-degenerate full-symmetric vibrations ν_1 (ν_s) at $1040\text{--}1110\text{ cm}^{-1}$; doubly degenerate symmetric bending vibrations ν_2 (δ_s) at $856\text{--}875\text{ cm}^{-1}$; triply degenerate asymmetric vibrations ν_3 (ν_{as}) at $1408\text{--}1490\text{ cm}^{-1}$; and triply degenerate bending vibrations ν_4 (δ_{as}) at $700\text{--}745\text{ cm}^{-1}$.

The other IR bands refer to the function-group composition of the organic component of the powders. All samples feature peaks at $2800\text{--}3000\text{ cm}^{-1}$, including the C–H stretching vibrations overlapping with N–H stretching vibrations, the latter being characteristic of bilirubin, lecithin, and amino acids. All spectra feature the band at $3200\text{--}3700\text{ cm}^{-1}$ due to the vibrations of the O–H bond involved in hydrogen bonding, characteristic of cholesterol and lecithin. At 2350 cm^{-1} there appear parasitic peaks of the C=O stretching vibrations in atmospheric carbon dioxide.

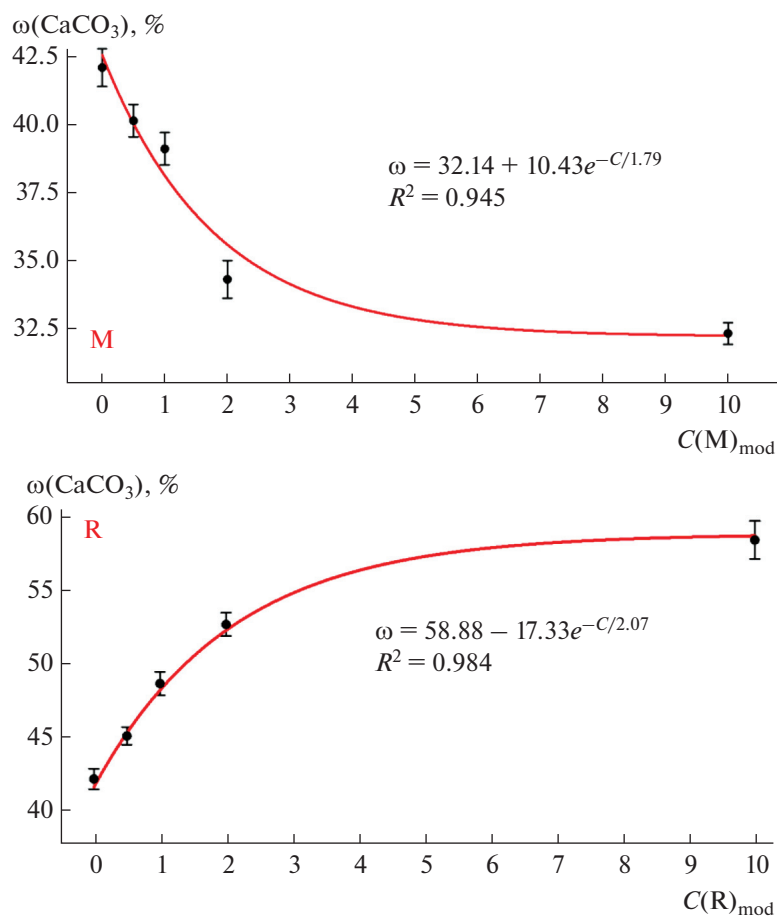


Fig. 1. CaCO_3 percentage (as Ca^{2+}) in the prepared samples versus Met (M) or Arg (R) concentrations in bile.

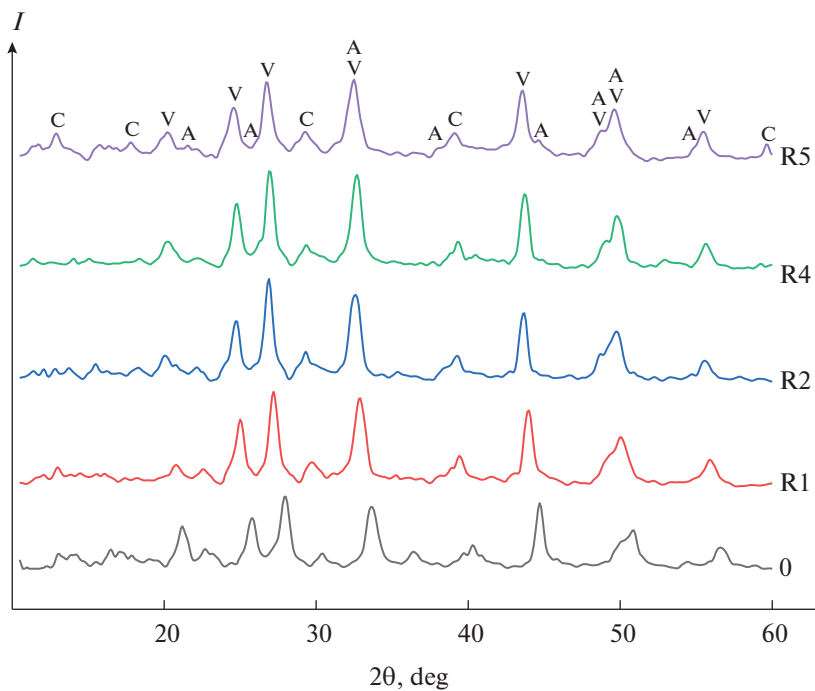


Fig. 2. X-ray diffraction patterns of CaCO_3 samples prepared in the presence of Arg in bile (A stands for aragonite, V for vaterite, and C for calcite).

Table 4. CaCO₃ percentages as Ca²⁺ determined complexometrically in prepared samples

Amino acid	C(AA)	Sample	$\omega(\text{CaCO}_3)$, %
Without AAs	0C _{mod}	01	42.9 ± 0.4
		02	41.2 ± 0.4
		Average	42.1 ± 0.7
His (H)	0.5C _{mod} 1C _{mod}	H1	43.6 ± 1.0
		H2	46.9 ± 0.9
		H3	46.3 ± 0.7
		Average	46.6 ± 0.5
	2C _{mod} 10C _{mod}	H4	52.2 ± 1.2
		H5	50.3 ± 1.6
Met (M)	0.5C _{mod} 1C _{mod}	M1	40.1 ± 0.6
		M2	38.4 ± 0.4
		M3	39.8 ± 0.5
		Average	39.1 ± 0.6
	2C _{mod} 10C _{mod}	M4	34.3 ± 0.7
		M5	32.3 ± 0.4
Arg (R)	0.5C _{mod} 1C _{mod}	R1	45.0 ± 0.6
		R2	48.2 ± 1.7
		R3	49.0 ± 0.9
		Average	48.6 ± 0.8
	2C _{mod} 10C _{mod}	R4	52.7 ± 0.8
		R5	58.5 ± 1.3
Trp (W)	0.5C _{mod} 1C _{mod}	W1	40.4 ± 0.8
		W2	35.6 ± 1.3
		W3	36.8 ± 1.4
		Average	36.2 ± 0.9
	2C _{mod} 10C _{mod}	W4	31.2 ± 1.7
		W5	32.9 ± 1.2
Average percentage over all samples			~ 42.7

In the range 1500–1600 cm⁻¹, there is a set of peaks due to the stretching vibrations of carboxylate ion O–C–O⁻ and the N–H bending vibrations in bilirubin and in NH₃⁺ in the amino acids.

Importantly, in the series of syntheses with Met or Trp, no significant qualitative changes are observed in the IR spectra of the prepared samples. In this case, the concentrations of the amino acids are insufficient for them to influence the structural-group composition of the prepared powders. In syntheses with His or Arg (Fig. 3), the amino acids cause a more pronounced effect: as the amino acid concentration in bile increases, the 875 cm⁻¹ and 1480–1490 cm⁻¹ vibrations grow in intensity; this growth is indicative of

an increase in the calcium carbonate percentage in the solid. The vibration band ν_3 acquires the form typical of aragonite, in correlation with the $\omega(\text{CaCO}_3)$ determination in the solid and the XRD results. The peaks of the bending vibrations in NH₃⁺ and the stretching vibrations in O–C–O⁻ at 1540–1640 cm⁻¹ also become stronger as the amino acid concentration rises. This trend may indicate an increase in the amount of the amino acid in the synthesized powders, where it can be present both in a free form in a mixture with amorphous and organic phases and in an adsorbed state on the surface of calcium carbonate crystals.

Optical microscopy confirms the results of all previous studies: spherulitic vaterite microparticles (up to ~10 μm) constitute the basis of all samples [2, 5].

In the samples prepared with His or Met, there are many agglomerated particles and amorphous inclusions of organic nature; the amount of vaterite spherulites decreases as the concentration of either of these amino acids in bile increases. The greatest amount of spherulitic vaterite particles is in the samples prepared in the presence of Arg or Trp (Fig. 4); the amount of these particles increases and their sizes decrease as the concentration of either of these amino acids in bile increases.

Photon correlation spectroscopy determined the sizes and volume fractions of particles in the <10 μm powder fractions. The results of measurements for each of the synthesized powders appear in Table 6 as confidence intervals. Most samples feature trimodal particle size distribution. Thus, the powders feature three fractions: fraction I comprises particles with radii of hundredths of a micrometer; fraction II comprises particles with radii of tenths of a micrometer; and fraction III comprises particles with micron-sized radii. Samples 01, 02, H1, H2, H3, M1, M4, and M5 have bimodal particle size distributions.

From the fraction compositions of the prepared CaCO₃ samples, one-way analysis of variance can elucidate correlation relations among the amino acid concentration in bile, particle size in every fraction, and the volume proportions of fractions in the general <10 μm fraction.

In the synthesis with His, the increasing amino acid concentration in bile gives rise to an increase in particle sizes in fractions II and III, a decrease in their proportions, and an increase in the proportion of fraction I (it appears in the precipitates when the histidine C_{mod} increases to 2C_{mod} and 10C_{mod}).

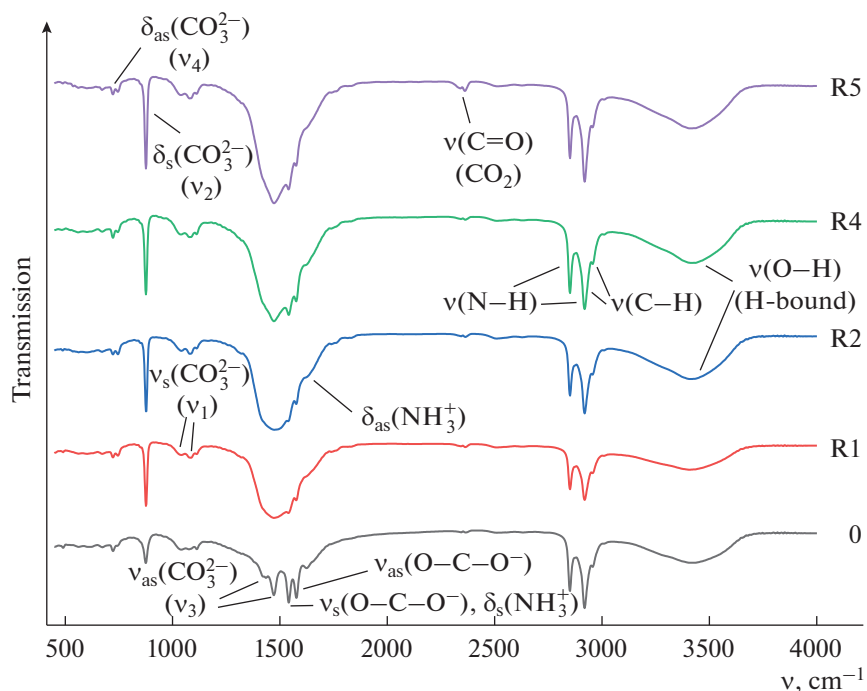
In the set of samples prepared with Met, fraction I appears only when the methionine concentration is 1C_{mod}. The particle size remains almost unchanged (it decreases only insignificantly after the jump at 1C_{mod}) as the Met concentration in bile increases, while the percentages of fractions II and III vary, experiencing a jump at 1C_{mod}.

Table 5. Phase compositions of samples (%) as determined by XRD (A stands for aragonite, V for vaterite, and C for calcite)

$C(AA)_{\text{mod}}$		$0C_{AA}$	$0.5C_{AA}$	$1C_{AA}$			$2C_{AA}$	$10C_{AA}$
Sample code		X0	X1	X2	X3	Average	X4	X5
Amino acid (X)	His (H)	85.0 V 12.5 A 2.5 C	80.7 V 12.5 A 6.8 C	92.1 V 7.5 A 0.4 C	87.4 V 7.5 A 5.1 C	89.8 V 7.5 A 2.7 C	89.5 V 3.0 A 7.5 C	88.8 V 3.7 A 7.5 C
	Met (M)		82.4 V 8.5 A 9.1 C	79.3 V 8.7 A 12.0 C	80.7 V 6.6 A 12.7 C	80.0 V 7.7 A 12.3 C	83.0 V 9.2 A 7.8 C	73.2 V 19.1 A 7.7 C
	Arg (R)		82.4 V 9.8 A 7.8 C	81.3 V 10.7 A 8.0 C	86.5 V 8.9 A 4.6 C	83.9 V 9.8 A 6.3 C	78.1 V 12.8 A 9.1 C	66.0 V 23.1 A 10.9 C
	Trp (W)		78.2 V 11.3 A 10.5 C	84.7 V 11.8 A 3.5 C	89.2 V 8.0 A 2.8 C	86.9 V 9.9 A 3.2 C	79.3 V 15.0 A 5.7 C	88.1 V 9.5 A 2.4 C

The samples prepared in the presence of Arg have the complete set of the three fractions. The particle radii remain almost unchanged as the amino acid concentration in bile increases, while the average particle size of fraction I reliably differs from the particle size obtained in the absence of amino acids. For fractions II and III, their proportions change in jump at $1C_{\text{mod}}$ arginine, with an increase in the proportion of fraction II and a decrease in the proportion of fraction III in response to a further addition of the AA.

The precipitates prepared with Trp feature fraction I, which is here reliably larger than in AA-free samples, while fractions I and II have their sizes almost unchanged, and fraction III has its size increasing, as Trp concentration increases. The proportion of fractions I and II decrease, while the proportion of fraction III increases as the Trp concentration in bile increases. The decrease in the proportion of a coarse-sized particle fraction and increase in the proportion of a fine-sized fraction can have an inhibitory effect on the growth and aggregation of the forming choleliths.

**Fig. 3.** IR spectra of CaCO_3 , samples prepared in the presence of Arg in bile.

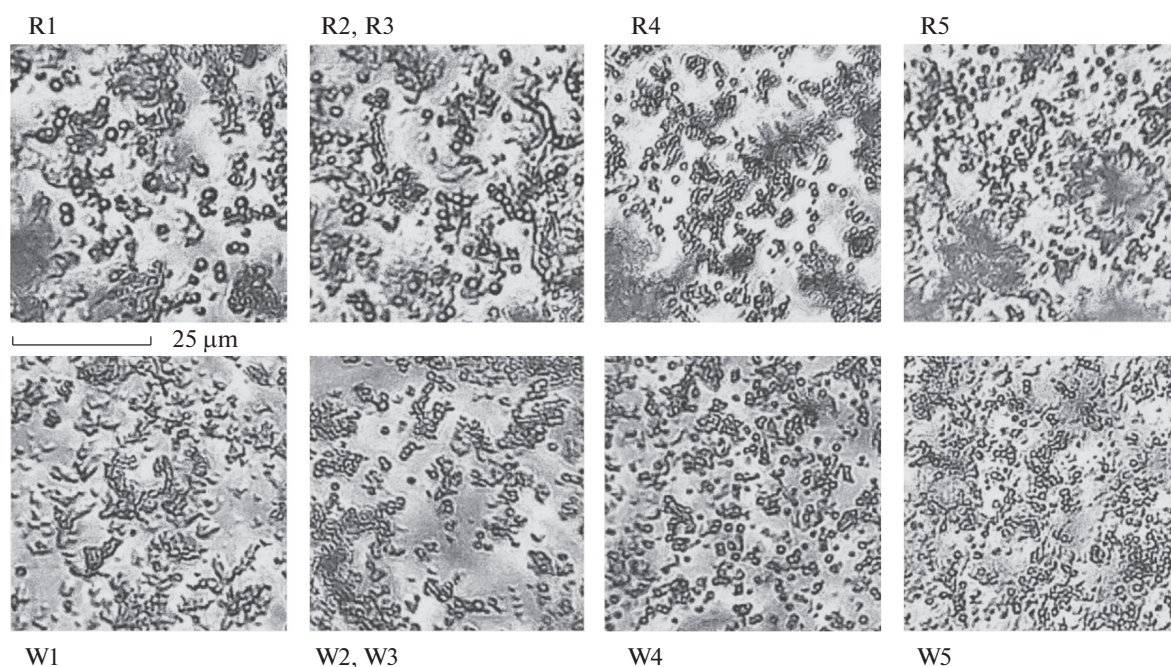


Fig. 4. Micrographs of CaCO_3 samples prepared in the presence of Arg and Trp.

Table 6. Particle radii (r) and their volume fractions (w) in samples

AA	$C(\text{AA})$	Sample	Fraction No.					
			I		II		III	
			$r, \mu\text{m}$	$w, \%$	$r, \mu\text{m}$	$w, \%$	$r, \mu\text{m}$	$w, \%$
Without AAs	$0C_{\text{mod}}$	01	—	—	0.14 ± 0.02	27.8 ± 5.6	4.6 ± 0.6	72.2 ± 7.9
		02	—	—	0.16 ± 0.02	29.8 ± 2.7	4.9 ± 0.3	70.2 ± 5.1
		Average	—	—	0.15 ± 0.01	28.8 ± 2.8	4.7 ± 0.3	71.2 ± 3.8
His (H)	$0.5C_{\text{mod}}$ $1C_{\text{mod}}$	H1	—	—	0.19 ± 0.01	47.1 ± 7.6	5.5 ± 0.5	52.9 ± 3.0
		H2	—	—	0.19 ± 0.02	41.1 ± 5.9	4.1 ± 0.5	58.9 ± 7.3
		H3	—	—	0.19 ± 0.01	39.8 ± 6.5	3.9 ± 0.4	60.2 ± 6.6
		Average	—	—	0.19 ± 0.01	40.4 ± 3.7	4.0 ± 0.2	59.6 ± 4.4
	$2C_{\text{mod}}$ $10C_{\text{mod}}$	H4	0.042 ± 0.006	8.8 ± 1.1	0.28 ± 0.04	49.6 ± 6.4	3.8 ± 0.7	41.6 ± 5.0
	H5	0.049 ± 0.002	23.4 ± 1.8	0.55 ± 0.05	36.9 ± 4.6	5.8 ± 0.3	39.7 ± 4.1	
Met (M)	$0.5C_{\text{mod}}$ $1C_{\text{mod}}$	M1	—	—	0.12 ± 0.02	23.7 ± 2.8	6.1 ± 0.8	76.3 ± 4.3
		M2	0.044 ± 0.011	12.9 ± 4.5	0.24 ± 0.03	47.0 ± 2.0	5.2 ± 0.8	40.1 ± 3.7
		M3	0.043 ± 0.007	12.8 ± 1.7	0.23 ± 0.03	50.9 ± 1.2	4.8 ± 0.8	36.3 ± 1.6
		Average	0.044 ± 0.005	12.9 ± 2.0	0.23 ± 0.02	48.9 ± 1.8	5.0 ± 0.5	38.2 ± 2.0
	$2C_{\text{mod}}$ $10C_{\text{mod}}$	M4	—	—	0.18 ± 0.02	35.3 ± 3.8	4.8 ± 0.7	64.7 ± 4.9
	M5	—	—	0.15 ± 0.01	26.1 ± 2.4	4.2 ± 0.4	73.9 ± 1.8	
Arg (R)	$0.5C_{\text{mod}}$ $1C_{\text{mod}}$	R1	0.055 ± 0.009	4.4 ± 0.9	0.24 ± 0.03	49.8 ± 4.5	4.8 ± 0.6	45.8 ± 2.9
		R2	0.039 ± 0.003	2.4 ± 0.4	0.21 ± 0.01	59.7 ± 1.4	3.5 ± 0.3	37.9 ± 1.9
		R3	0.031 ± 0.009	3.2 ± 0.8	0.22 ± 0.03	57.0 ± 3.0	3.7 ± 0.4	39.8 ± 2.1
		Average	0.034 ± 0.006	2.3 ± 0.3	0.22 ± 0.01	58.4 ± 2.3	3.6 ± 0.2	38.8 ± 1.2
	$2C_{\text{mod}}$ $10C_{\text{mod}}$	R4	0.035 ± 0.007	1.8 ± 0.4	0.21 ± 0.03	40.3 ± 4.1	4.6 ± 0.5	57.9 ± 2.4
	R5	0.039 ± 0.004	6.0 ± 1.5	0.23 ± 0.04	36.4 ± 4.5	4.1 ± 0.4	57.7 ± 3.5	
Trp (W)	$0.5C_{\text{mod}}$ $1C_{\text{mod}}$	W1	0.036 ± 0.003	8.3 ± 1.1	0.27 ± 0.03	36.9 ± 3.4	7.0 ± 0.4	54.8 ± 2.8
		W2	0.053 ± 0.006	2.3 ± 0.7	0.22 ± 0.01	43.3 ± 3.8	7.8 ± 1.3	54.4 ± 6.4
		W3	0.045 ± 0.005	1.8 ± 0.4	0.24 ± 0.01	46.1 ± 5.2	7.0 ± 0.9	52.1 ± 3.4
		Average	0.049 ± 0.004	2.1 ± 0.4	0.23 ± 0.01	44.7 ± 2.8	7.4 ± 0.7	53.2 ± 3.1
	$2C_{\text{mod}}$ $10C_{\text{mod}}$	W4	0.042 ± 0.001	1.8 ± 0.6	0.25 ± 0.03	38.6 ± 4.5	7.1 ± 1.1	59.6 ± 4.9
	W5	0.042 ± 0.004	16.2 ± 1.7	0.26 ± 0.02	46.7 ± 1.7	9.1 ± 1.3	37.1 ± 2.6	

CONCLUSIONS

Twenty two calcium carbonate samples altogether have been prepared in bile with variable concentrations of the amino acid His, Met, Arg, or Trp.

The calcium percentage was determined as CaCO₃ in the solid phases by complexometric titration in all prepared samples. The samples prepared with Arg have the highest CaCO₃ yield, while those prepared with Met have the lowest CaCO₃ yield. The increasing amino acid concentration gives rise to an increase in the calcium carbonate weight fraction in the syntheses with His or Arg and to a decrease in the syntheses with Met or Trp. An inhibitory effect of Met is noticed on CaCO₃ crystallization and on precipitation in bile in general.

Vaterite is the major component of the phase composition in all of the powders prepared as shown by XRD. Met and Arg have been shown to have a stabilizing effect on metastable aragonite: as their concentration in bile increases, the aragonite weight fraction in the solid increases, too. This can have an inhibitory effect on the subsequent growth and aggregation of gallstones, for aragonite differs from vaterite in morphology, zeta potential, and thereby adhesion to cholesterol. The results of FT-IR spectroscopy correlate with XRD data.

Optical microscopy showed vaterite spherulites in all prepared powders. Photon correlation spectroscopy has shown that calcium carbonate particles with radii less than 10 μm are represented by three fractions. Of greatest interest are the syntheses with His and Trp, in which the proportion of the small-sized fraction increases and the proportions of coarse-sized fractions decrease as the amino acid concentration rises. With this, the particle radius increases in all fractions.

The results signify the necessity of further studies into mineralization in human bile on model systems in order to identify mechanisms, elucidate correlation relations, and determine causes for gallstone nucleation. In the future, we intend to study the effect of the amino acids considered in this work on the composition and properties of CaCO₃ in another range of concentrations and in their joint presence.

CONFLICT OF INTEREST

The authors declare that they have no conflicts of interest.

REFERENCES

1. D. G. Tikhonov, Yakut. Med. Zh. **4**, 91 (2015).
2. O. A. Golovanova and S. S. Leonchuk, Russ. J. Inorg. Chem. **65**, 449 (2020).
<https://doi.org/10.1134/S0036023620040063>
3. A. C. Guyton and J. E. Hall, *Textbook of Medical Physiology* (Elsevier Inc., 2006).
4. L. N. Poloni and M. D. Ward, Chem. Mater. **26**, 477 (2014).
<https://doi.org/10.1021/cm402552v>
5. N. A. Pal'chik, V. N. Stolpovskaya, T. N. Moroz, et al., Russ. J. Inorg. Chem. **48**, 1921 (2003).
6. E. V. Mashina, B. A. Makeev, and V. N. Filippov, Izv. Tomsk. Politekh. Univ. **326**, 34 (2015).
7. O. A. Golovanova and S. S. Leonchuk, Vestnik Omsk Gos. Univ. **24**, 66 (2019).
[https://doi.org/10.25513/1812-3996.2019.24\(2\).66-73](https://doi.org/10.25513/1812-3996.2019.24(2).66-73)
8. M. W. Neubrand, M. C. Carey, and T. M. Laue, Biochemistry **54**, 6783 (2015).
<https://doi.org/10.1021/acs.biochem.5b00874>
9. O. A. Sablin, V. B. Grinevich, Yu. P. Uspenskii, et al., *Functional Diagnostics in Gastroenterology* (VMedA, St. Petersburg, 2002).
10. C.-Y. Cheng, H. Oh, T.-Y. Wang, et al., Langmuir. **30**, 10221 (2014).
<https://doi.org/10.1021/la502380q>
11. M. M. H. Al Omari, I. S. Rashid, N. A. Qinna, et al., *Profiles of Drug Substances, Excipients, and Related Methodology*, vol. 41 (Academic Press, Burlington, 2016).
<https://doi.org/10.1016/bs.podrm.2015.11.003>
12. E. Ros, S. Navarro, I. Fernandez, et al., Gastroenterology **91**, 703 (1986).
[https://doi.org/10.1016/0016-5085\(86\)90642-6](https://doi.org/10.1016/0016-5085(86)90642-6)
13. J.-K. Yu, H. Pan, S.-M. Huang, et al., Asian J. Surgery **36**, 26 (2013).
<https://doi.org/10.1016/j.asjsur.2012.06.001>
14. L. Poudel, C. Tamerler, A. Misra, et al., J. Phys. Chem. **121**, 28354 (2017).
15. I. I. Klimovich, E. M. Doroshenko, V. P. Strapko, et al., Zh. Grod. Gos. Med. Univ. **1**, 14 (2008).
16. D. Evans, P. B. Webb, K. Penkman, et al., Cryst. Growth Des. **19**, 4300 (2019).
<https://doi.org/10.1021/acs.cgd.9b00003>
17. S. W. Lee and C. S. Choi, Cryst. Growth Des. **7**, 1463 (2007).
<https://doi.org/10.1021/cg0700420>
18. M. A. Trubitsyn, H. V. Hung, L. V. Furda, et al., Russ. J. Inorg. Chem. **66**, 654 (2021).
<https://doi.org/10.1134/S0036023621050211>
19. N. A. Zakharov, E. M. Koval, A. D. Aliev, et al., Russ. J. Inorg. Chem. **66**, 305 (2021).
<https://doi.org/10.1134/S0036023621030219>
20. O. A. Golovanova, Russ. J. Inorg. Chem. **65**, 305 (2021).
<https://doi.org/10.1134/S0036023620030043>
21. R. F. Fakhrullin, A. G. Bikmullin, and D. K. Nurgaliev, ACS Appl. Mater. Interfaces **1**, 1847 (2009).
<https://doi.org/10.1021/am9003864>
22. N. Serov, D. Darmoroz, A. Lokteva, et al., Chem. Commun. **56**, 11969 (2020).
<https://doi.org/10.1039/DOCC05502F>
23. W.-T. Hou and Q.-L. Feng, Cryst. Growth Des. **6**, 1086 (2006).
<https://doi.org/10.1021/cg0504861>
24. V. Lauth, B. Loretz, C.-M. Lehr, et al., Chem. Mater. **28**, 3796 (2016).
<https://doi.org/10.1021/acs.chemmater.6b00769>

25. T. T. Berezov and B. F. Korovkin, *Biological Chemistry* (Meditsina, Moscow, 1998) [in Russian].
26. M. A. Hood, K. Landfester, and R. Munoz-Espi, *Cryst. Growth Des.* **14**, 1077 (2014).
<https://doi.org/10.1021/cg401580y>
27. R. Murray, D. Granner, P. Mayes, and V. Rodwell, *Harper's Illustrated Biochemistry*, 27th Ed. (Mc Graw-Hill Medical Publishing, 2006).
28. K. Nakamoto, *Infrared and Raman Spectra of Inorganic and Coordination Compounds* (Wiley Online Library, 2008).
<https://doi.org/10.1002/9780470405840>
29. N. B. Egorov and V. V. Shagalov, *Infrared Spectroscopy of Rare and Scattered Elements* (Izd-vo TPU, Tomsk, 2012) [in Russian].
30. R. M. Silverstein, F. X. Webster, J. K. David, et al., *Spectrometric Identification of Organic Compounds* (Wiley, 2014).
31. V. S. Kurazhkovskaya and E. Yu. Borovikova, *Infrared and Mössbauer Spectroscopy of Crystals* (Moscow State Univ., Moscow, 2008) [in Russian].

Translated by O. Fedorova